

# Filling the gap in the IERS C01 polar motion series in 1858.9–1860.9

Zinovy Malkin<sup>1</sup>, Nina Golyandina<sup>2</sup>, Roman Olenev<sup>3</sup>

<sup>1</sup>Pulkovo Observatory, St. Petersburg, 196140, Russia, malkin@gaoran.ru

<sup>2</sup>Faculty of Mathematics and Mechanics, St. Petersburg State University,  
St. Petersburg, 199034, Russia, n.golyandina@spbu.ru

<sup>3</sup>Faculty of Mathematics and Mechanics, St. Petersburg State University,  
St. Petersburg, 199034, Russia, roman.olenov.cs@mail.ru

February 2, 2025

## Abstract

The C01 Earth orientation parameters (EOP) series provided by the International Earth Rotation and Reference Systems Service (IERS) is the longest reliable record of the Earth’s rotation. In particular, the polar motion (PM) series beginning from 1846 provides a basis for investigation of the long-term PM variations. However, the pole coordinate  $Y_p$  in the IERS C01 PM series has a 2-year gap, which makes this series not completely evenly spaced. This paper presents the results of the first attempt to overcome this problem and discusses some ways to fill this gap. Two novel approaches were considered for this purpose: parametric astronomical model consisting of the bias and the Chandler and annual wobbles with linearly changing amplitudes, and data-driven model based on Singular Spectrum Analysis (SSA). Both methods were tested with various options to ensure robust and reliable results. The results obtained by the two methods generally agree within the  $Y_p$  errors in the IERS C01 series, but the results obtained by the SSA approach can be considered preferable because it is based on a more complete PM model.

## 1 Introduction

Time series of the Earth orientation parameters (EOP) are the main source of information for investigation of the Earth’s rotation, in particular the motion of the Earth’s rotation axis in the terrestrial reference frame, which is also called polar motion (PM). Historical overview of the PM observations and analyses can be found in Dick et al. (2000). The PM is a complex phenomenon, which consists of many variational components including trends and (quasi)periodical oscillations with periods from several hours to several decades. In particular, the study of long-term polar motion variations is crucial for expanding our understanding of Earth’s dynamic processes, particularly in terms of the impacts of climate change, changes in Earth’s internal structure and the redistribution of global mass. To study slow PM variations, long time series of the pole coordinates  $X_p$  and  $Y_p$  is needed. The longer the time interval covered by EOP series, the lower frequency variations can be detected and investigated.

The international standard of the EOP series is the combined series computed by the International Earth Rotation and Reference Systems Service (IERS) (Bizouard et al., 2019). The IERS C01 EOP series contains the longest PM series derived from astronomical observations lasting from 1846 to

Table 1: Content of the IERS C01 polar motion series.

Date interval	Data source
1846 – 1889	Rykhlova (1970a)
1890 – 1899	Fedorov et al. (1972)
1900 – 1961	Vondrák et al. (1995, 2010)
1962 – now	Bizouard et al. (2019)

now<sup>1</sup>. It is widely used for analysis of the decadal variations in Earth’s rotation (Gaposchkin, 1972; Vondrák, 1988; Rykhlova and Kurbasova, 1990; Kołaczek and Kosek, 1999; Gambis, 2000; Yatskiv, 2000; Schuh et al., 2001; Höpfner, 2004; Guo et al., 2005; Malkin and Miller, 2010; Vityazev et al., 2010; Zotov, 2010; Miller, 2011; Seitz et al., 2012; Zotov and Bizouard, 2012; Beutler et al., 2020; Lopes et al., 2022; Zotov et al., 2022; Yamaguchi and Furuya, 2024).

However, the IERS PM series has a 2-year gap in  $Y_p$  pole coordinate in the date range 1858.8 to 1861.0. Of course, a time series without missing epochs is always better than a series with a gap. Missing data can cause problems in statistical data analysis. In particular, for spectral analysis, most of the standard methods used require continuous regularly spaced data. If the latter is the case, the results are free from the risk of introducing spurious frequencies in the spectrum. It is also possible to use other efficient analysis methods for regularly spaced data. The reconstructed continuous evenly spaced PM series can also provide new information about the evolution of the Earth’s rotation modes in the gap epochs.

In this paper, for the first time, to our knowledge, we examine some approaches to address the problem of filling the gap in the IERS C01 series. The challenge is to fill in the missing  $Y_p$  values in the series while preserving its structure as much as possible. For this purpose, two methods of analysis were considered. The first is the use of a parametric astronomical model, specially developed for this study and consisted of three components: bias, Chandler wobble (CW), and annual wobble (AW) (hereafter referred to as BCA model). The second data-driven model has been constructed using Singular Spectrum Analysis (SSA) (Golyandina et al., 2001). These two methods cover the range of models, from parametric to nonparametric, and allow the treatment of time series that do not have a single fundamental period and are rather short.

The paper is organized as follows. Section 2 describes the data used in this study and presents the results of its preliminary analysis. Section 3 is devoted to deriving a parametric model of the IERS C01 series. A refined analysis of the IERS C01 PM series using the SSA technique is performed in Section 4. Details of SSA analysis are described in Appendix A. Section 5 sums up the results obtained in this work. Concluding remarks on this study are given in the final Section.

## 2 Data description and preliminary analysis

The IERS C01 PM series consists of several parts as described in Table 1. The epoch step in this series is 0.1 yr in 1846—1890, and 0.05 yr starting with 1890. In this study, the beginning of the IERS C01 series in the date range 1846 to 1899 was used. Corresponding PM data are shown in Fig. 1

In this study, we have focused on the 19th century part of the IERS C01 PM series, primarily on the period 1846–1889. Although the pole coordinates related to the 19th century have relatively low accuracy compared to PM data obtained after 1900, they are of great importance for investigation

<sup>1</sup><ftp://hpiers.obspm.fr/iers/eop/eopc01/eopc01.iau2000.1846-now>

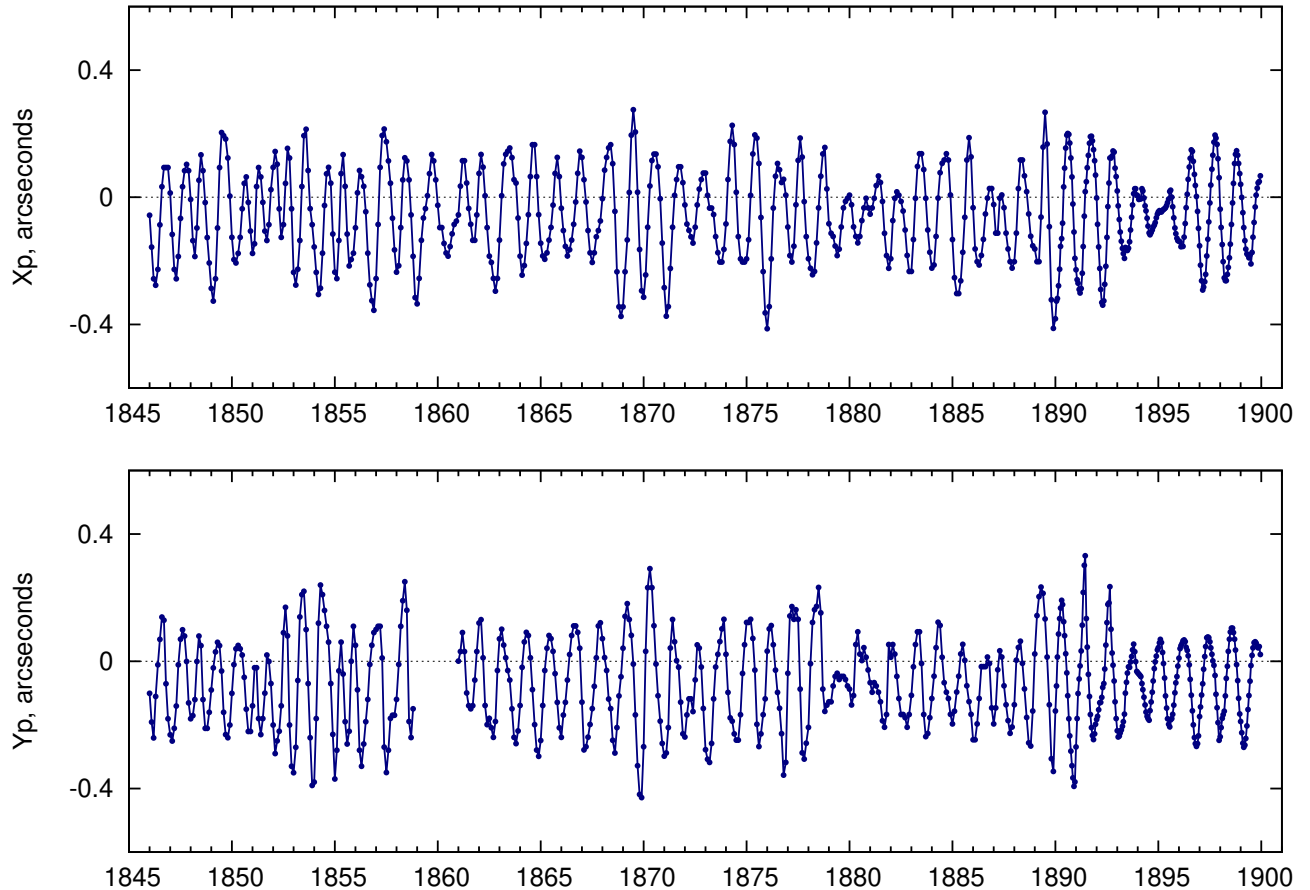


Figure 1: The  $X_p$  component (top panel) and  $Y_p$  component (bottom panel) of the IERS C01 series.

of long-term variations the Earth's rotation. Suffice it to say that as early as the late 19th century Chandler (1894a) separated CW and AW signals, derived the value of the CW period of 428-430 days, which is close to the latter determinations, and discovered an  $\approx 66$ -year period of the CW amplitude variation, which is only about 20% shorter than recently obtained from 180-year PM series. Including the 19th century PM data into modern analyses of the entire IERS C01 PM series provides good evidence for 80-year CW periodicity in amplitude and phase variations, which cannot be reliably estimated using only observations since 1900. All this certainly confirms how useful the 19th century PM series are for studying long-term behavior of the PM.

While the work of Fedorov et al. (1972) is widely available and well documented, the original work Rykhlova (1970a) is less known and available and it makes sense to briefly describe it here. This work was based on the analysis of latitude determinations that were made in the framework of several programs for determination of absolute declinations of stars at three observatories: Greenwich, Pulkovo, and Washington. The Greenwich latitude variations were taken from Chandler (1894b) (years 1836.0–1851.0) and Thackeray (1893) (years 1851.0–1891.5). The Pulkovo latitude variations were taken from Orlov (1961) (years 1842.0–1849.5, 1863.6–1879.0, and 1882.0–1892.0). The Washington latitude variations were derived in Rykhlova (1970b) (years 1845.1–1858.8 and 1861.0–1888.0). All three stations were given equal weights.

The pole coordinates were computed using the formula

$$\Delta\varphi = X_p \cos \lambda + Y_p \sin \lambda, \quad (1)$$

where  $\lambda$  is the latitude of observatory. For most epochs of the Rykhlova PM series, data from all three observatories were used. In the period when Pulkovo was not observing, the pole coordinates were computed using data from Greenwich and Washington. In the Rykhlova series and, consequently, the IERS C01 PM series there are no  $Y_p$  data from 1858.9 to 1860.9 inclusive. A total of 21 epochs are missing. The middle epoch of the gap is 1859.9. The gap is explained by absence of observations at Washington observatory during this period. The problem is that the Greenwich and Pulkovo observatories are located at close longitudes,  $0^\circ$  and  $30^\circ$ , respectively, which is close to direction of  $X_p$ . Therefore, it is impossible to accurately estimate the both pole coordinates using only observations from these two stations. Consequently, only  $X_p$  values were computed for these epochs. The Washington observatory is located at longitude  $-77^\circ$ , which is close to the  $Y_p$  direction, and its inclusion in the processing provides a good longitude coverage to reliably determine both pole coordinates.

Although the polar motion variations described by the IERS C01 series for 1846–1899 are assumed to consist mainly of AW and CW components, possibly with bias<sup>2</sup>, spectral analysis has shown that in fact the signal has a more complex structure as shown in Fig. 2. The generalized Lomb-Scargle periodograms for the C01  $X_p$  and  $Y_p$  series were computed according to Zechmeister and Kürster (2009) after removing the bias clearly visible in Fig. 1.

### 3 Parametric model

It is not possible to use a straightforward model consisting of two components, CW and AW, because their amplitudes do not remain constant over time in the date range around the gap (Kołaczek and Kosek, 1999; Yatskiv, 2000; Guo et al., 2005; Miller, 2011; Lopes et al., 2022; Zotov et al., 2022). However, these two independent analyses of the IERS C01 series showed that the CW amplitude grew nearly linearly in 1850–1870. Miller (2011) also showed that the AW amplitude is nearly constant in this period with a tiny increase over time. Therefore, it is possible to construct an approximation model for  $X_p$  and  $Y_p$  for the period around 1850–1870, consisting of a bias and two oscillations with CW and AW periods and linear amplitude trend:

$$\begin{aligned} Y_p = & a_0 \\ & + (1 + a_1^c t) \left( a_c^c \cos \frac{2\pi(t - t_0)}{P_c} + a_s^c \sin \frac{2\pi(t - t_0)}{P_c} \right) \\ & + (1 + a_1^a t) \left( a_c^a \cos \frac{2\pi(t - t_0)}{P_a} + a_s^a \sin \frac{2\pi(t - t_0)}{P_a} \right), \end{aligned} \quad (2)$$

---

<sup>2</sup><ftp://hpiers.obspm.fr/iers/eop/eopc01/EOPC01.GUIDE>

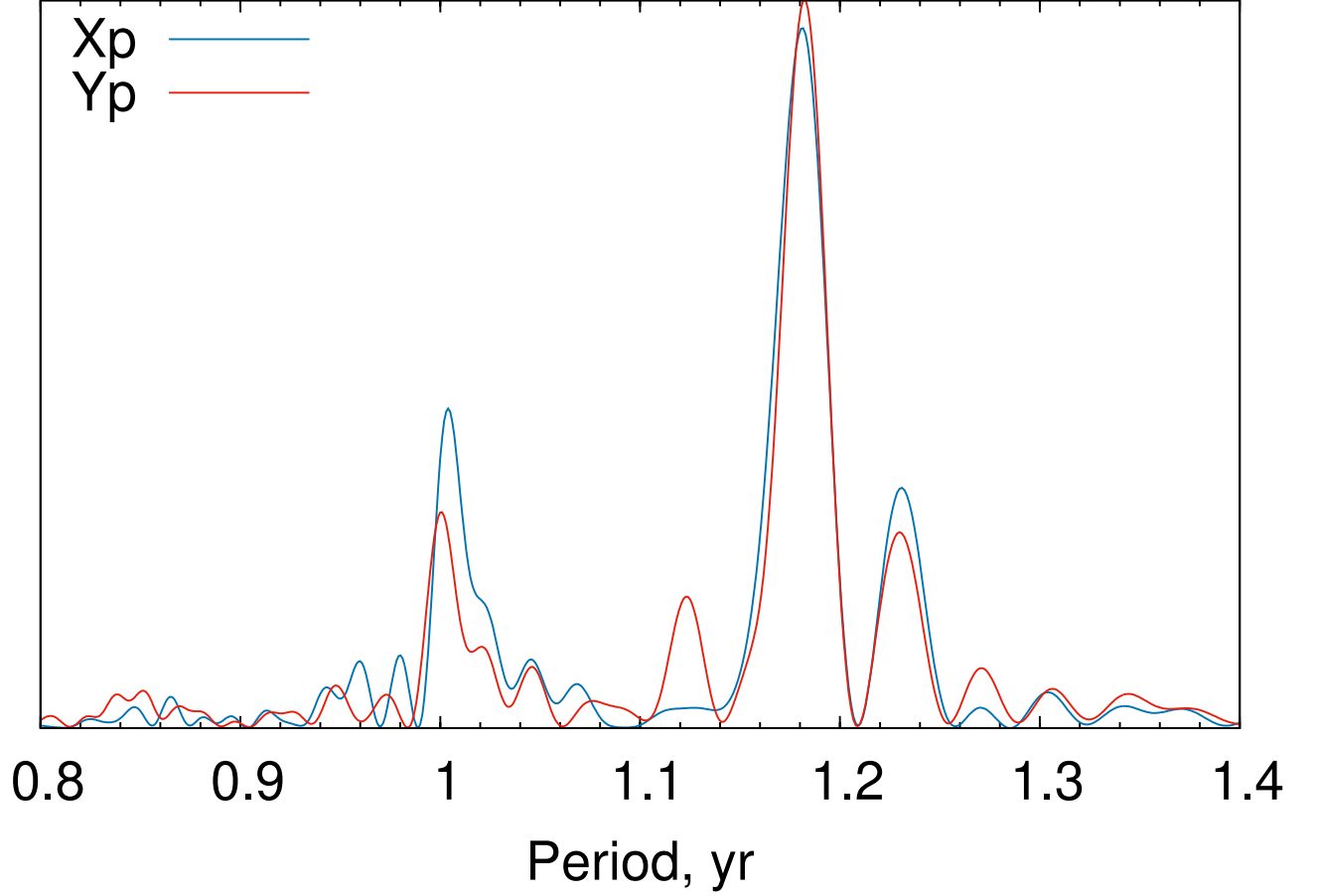


Figure 2: Generalized Lomb-Scargle periodogram of the IERS C01 PM series for the interval 1846–1899, arbitrary units.

or, equivalently,

$$\begin{aligned}
Y_p = & a_0 \\
& + a_{c0}^c \cos \frac{2\pi(t-t_0)}{P_c} + a_{s0}^c \sin \frac{2\pi(t-t_0)}{P_c} \\
& + a_{c1}^c t \cos \frac{2\pi(t-t_0)}{P_c} + a_{s1}^c t \sin \frac{2\pi(t-t_0)}{P_c} \\
& + a_{c0}^a \cos \frac{2\pi(t-t_0)}{P_a} + a_{s0}^a \sin \frac{2\pi(t-t_0)}{P_a} \\
& + a_{c1}^a t \cos \frac{2\pi(t-t_0)}{P_a} + a_{s1}^a t \sin \frac{2\pi(t-t_0)}{P_a},
\end{aligned} \tag{3}$$

where  $t$  is epoch in years,  $t_0=1859.9$  (the middle epoch of the gap),  $P_c=1.19$  yr is the period of the CW, and  $P_a=1$  yr is the period of the AW.

The nine parameters of this model were fitted using the least squares method (LS) over seven intervals of length of 12 to 24 years with a step of 2 years centered at the middle epoch of the gap in  $Y_p$  series, 1859.9, in total seven variants. Then the filling  $Y_p$  values were computed using this model for each variant. The results of these computations are shown in Fig. 3 (upper panel).

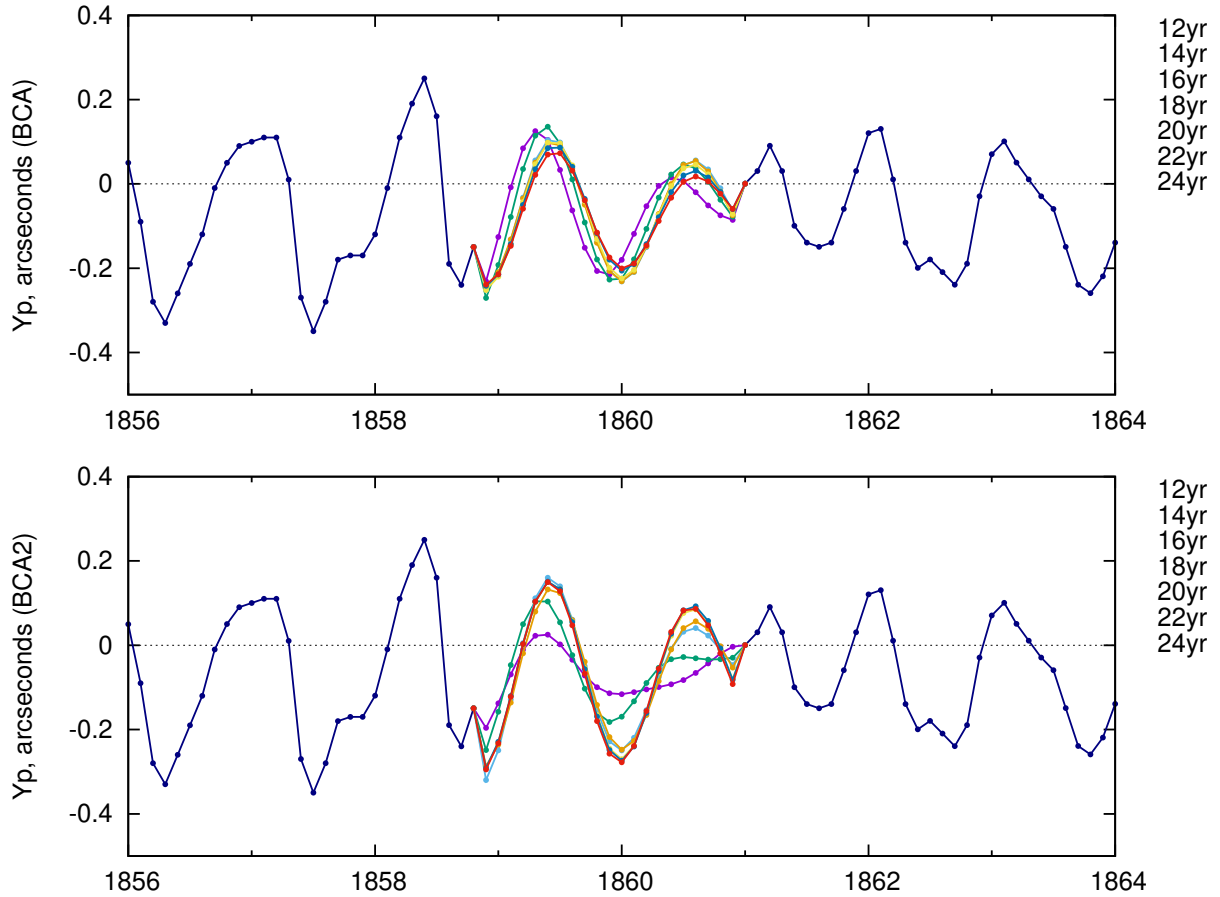


Figure 3: IERS C01  $Y_p$  series with filled missed data between 1858.9 and 1860.9 using the BCA model (upper panel) and BCA2 (bottom panel). Plot titles show date intervals used to fit the  $Y_p$  data to the model.

The BCA model represented by Eq. 3 corresponds to the PM model with a single dominant CW frequency, which is generally accepted at present. However, the PM spectrum presented in Fig. 2 reveals two peaks in the CW frequency band with periods of 1.181 yr and 1.231 yr. There may be various reasons for this bifurcation of the PM spectrum, such as an inconsistency in the data on which the series is based, or CW phase variations. In any case, it would be interesting to check how this effect may affect the result of the computation of the modeled  $Y_p$  in the gap.

For this purpose, the BCA2 model was constructed as follows:

$$\begin{aligned}
Y_p = & a_0 \\
& + a_{c0}^{c1} \cos \frac{2\pi(t-t_0)}{P_{c1}} + a_{s0}^{c1} \sin \frac{2\pi(t-t_0)}{P_{c1}} \\
& + a_{c1}^{c1} t \cos \frac{2\pi(t-t_0)}{P_{c1}} + a_{s1}^{c1} t \sin \frac{2\pi(t-t_0)}{P_{c1}} \\
& + a_{c0}^{c2} \cos \frac{2\pi(t-t_0)}{P_{c2}} + a_{s0}^{c2} \sin \frac{2\pi(t-t_0)}{P_{c2}} \\
& + a_{c1}^{c2} t \cos \frac{2\pi(t-t_0)}{P_{c2}} + a_{s1}^{c2} t \sin \frac{2\pi(t-t_0)}{P_{c2}} \\
& + a_{c0}^a \cos \frac{2\pi(t-t_0)}{P_a} + a_{s0}^a \sin \frac{2\pi(t-t_0)}{P_a} \\
& + a_{c1}^a t \cos \frac{2\pi(t-t_0)}{P_a} + a_{s1}^a t \sin \frac{2\pi(t-t_0)}{P_a},
\end{aligned} \tag{4}$$

where  $t$  is epoch in years,  $t_0=1859.9$  (the middle epoch of the gap),  $P_{c1}=1.181$  yr is the period of the first CW component,  $P_{c2}=1.231$  yr is the period of the second CW component, and  $P_a=1$  yr is the period of the AW. In this case, a longer interval of dates is needed to separate the two CW components. The 13 parameters of this model were fitted using the least squares method (LS) over seven intervals of length of 12 to 24 years with a step of 2 years centered at the middle epoch of the gap in  $Y_p$  series, 1859.9,. The fitting  $Y_p$  values for the BCA2 model are shown in Fig. 3 (bottom panel). They are close to the results obtained with the BCA model.

To evaluate the real accuracy of the PM series approximation by the parametric models, we computed the differences between the modeled and observed PM values for each of seven variants for the epochs before and after the gap. Then we computed the root mean square error (RMSE) and mean absolute error (MAE) for these differences. The same computations were repeated for the  $X_p$  series, for which we used the original IERS C01 series from which the epochs 1858.9–1860.9 were cut to make it similar to the  $Y_p$  series. The results of this error analysis are shown in Table 2. Two main observations can be made from this table. First, shorter intervals provide better approximation, as expected. Secondly, the approximation error for the  $X_p$  series is better than for the  $Y_p$  series, which corresponds to a higher precision of the  $X_p$  values with respect to the  $Y_p$  values given in the IERS C01 series in the 19th century. Although the approximation error for the BCA2 model is better than that for the BCA model, the latter may be more significant from a scientific point of view because a duality of the CW period is doubtful. For this reason, the average of two first BCA variants and two first BCA2 variants, i.e. those obtained for 12-year and 14-year variants, hereafter referred to as BCA model, will be used for further comparisons.

Generally speaking, other advanced models can be constructed in a similar way with more complicated behavior of trend, and CW and AW amplitudes (and maybe phases), but such an extension does not look reasonable in our case because there is no data enough to fit a many-parameter model. Therefore, analysis based on the BCA model cannot provide a fully satisfactory solution because it relies on a model that only approximately describes the actual pole motion. However, it may be useful for verification of other models. The more reliable solution to the problem to which this study is aimed will be obtained in the next Section using the data-driven SSA technique.

Table 2: Approximation error for the parametric models BCA and BCA2.

Interval of dates	$X_p$		$Y_p$	
	MAE	RMSE	MAE	RMSE
BCA model				
1853.89–1865.91	0.068	0.081	0.067	0.090
1852.89–1866.91	0.066	0.081	0.071	0.095
1851.89–1867.91	0.079	0.099	0.084	0.110
1850.89–1868.91	0.077	0.096	0.083	0.108
1849.89–1869.91	0.078	0.097	0.084	0.111
1848.89–1870.91	0.079	0.098	0.087	0.112
1847.89–1871.91	0.079	0.098	0.085	0.110
BCA2 model				
1853.89–1865.91	0.062	0.076	0.060	0.084
1852.89–1866.91	0.064	0.078	0.060	0.085
1851.89–1867.91	0.073	0.091	0.070	0.095
1850.89–1868.91	0.073	0.092	0.076	0.102
1849.89–1869.91	0.071	0.089	0.077	0.102
1848.89–1870.91	0.071	0.088	0.075	0.099
1847.89–1871.91	0.073	0.092	0.076	0.100

## 4 SSA analysis

The SSA method is one of the most powerful tools for analyzing time series with a complex structure including the PM series (Vautard and Ghil, 1989; Elsner and Tsonis, 1996; Golyandina et al., 2001; Ghil et al., 2002; Vityazev et al., 2010; Miller, 2011; Golyandina and Zhigljavsky, 2020). It is widely used for analyzing geodetic, geophysical, and astronomical time series, in particular, for filling gaps in time series (Kondrashov and Ghil, 2006; Golyandina and Osipov, 2007; Shen et al., 2015; Okhotnikov and Golyandina, 2019; Yi and Sneeuw, 2021; Ji et al., 2023). SSA is an agile method because it can propose a (possibly local) approximation by a model in the form of a finite sum of products of polynomials, exponentials and harmonics. This model is called linear because it consists of signals governed by linear recurrence relations. However, this is a rather large class of signals, and a signal may only approximately satisfy the model. This means that within a two-year time frame, this property of SSA overcomes its limitations. It should be noted that the set of frequencies does not change during the time interval considered, but rather their amplitudes. By varying the window length, SSA can account for amplitude changes even in the case of some non-linearity.

For further presentation of our method, we denote IERS C01 PM coordinates  $X_p$  and  $Y_p$  as  $X$  and  $Y$ , respectively. As in the case of the parametric model considered in Section 3, we will consider a model in the form of signal plus noise, assuming that the signal consists of three main components: trend, AW, and CW, with possible addition of other smaller components. Unlike parametric model specification, in the SSA method, the model does not need to be specified in advance, including setting the component periods. The signal components are defined adaptively by the SSA method and, as will be shown further on, are indeed composed of the listed components. We will process the PM time series with 10 measurements per year. Thus, the AW component corresponds to a period of 10 points, and the CW component corresponds to a period of about 11.9 points. Unlike the parametric BCA model described above, the SSA analysis does not imply a priori restrictions on the trend, AW

and CW variations. The general approach to gap filling with SSA is described in Appendix A.

In the real form, the SSA method works well with signals as a sum of possibly modulated harmonics (Golyandina et al., 2001). Such a modification of SSA applied to a single time series  $Y$  will be called hereafter 1D-SSA.

It was shown in Golyandina et al. (2015) that if several signals have the same periods (with the same modulation), Multivariate SSA (MSSA), a generalization of SSA for time series system analysis, extracts the signal more accurately. Such a method allows us to process  $X$  and  $Y$  series together.

Taking into account the physical nature of the pole coordinates, this looks reasonable to consider a representation of the PM series as a complex-valued time series and applied Complex SSA (CSSA). If the input signal consists of two harmonics with a phase shift of  $\pi/2$ , then CSSA extracts the signal even more accurately Golyandina et al. (2015).

To ensure more reliable results, we considered the three methods described above for reconstruction of PM signal: basic 1D-SSA for the series  $Y$ , MSSA for the series  $(X, Y)$ , and CSSA for the series  $X+iY$ . Note that MSSA and CSSA are applied to both time series,  $X$  and  $Y$ , together, so they take into account the relationships between the series. The methods MSSA and CSSA result in decompositions of both series, but we will use only the part of the decomposition of the series  $Y$ .

An important option for a practical SSA realization is a choice of the window length. Recommendations for optimal window selection include proportionality to the periods of the harmonics we want to extract (Golyandina et al., 2001). Therefore, for the window length  $L$  we will consider three values, 60, 119 and 238 points, since the AW and CW periods, 1.0 and 1.19 yr, respectively, are included near integer number of times in windows of this length.

The parameter that we want to optimize using artificial gaps is  $r$ , the number of the SVD components assigned to the signal. We will call  $r$  the model order. To find the optimal value of the model order, we vary it from 1 to 17 and calculate the error of gap filling according to Algorithm 1. We again used RMSE and MAE as a measure of the difference between the imputed values and the input time series values.

As a set of artificial gaps, we considered  $R = 120$  gap intervals of length  $M = 21$ , the same as the actual gap. The first interval starts at 1846.1, the remaining 119 intervals are obtained by successively shifting the initial interval four points forward (intervals with actual gaps were excluded).

The mean MAE and RMSE errors for these models are presented in Table 3. These test results have shown that the most precise filling of artificial gaps were achieved using CSSA with  $(L=60, r=4, 5)$ ,  $(L=119, r=6-9)$ ,  $(L=238, r=7)$ . These seven variants provide practically the same error of the approximation of the  $Y$  series. Similar results were obtained for RMSE, for which the optimal parameters  $r$  and  $L$  turned out to be the same as for the MAE estimate. Thus, it has been found that the obtained conclusions do not depend on the choice of the method for estimating the modeling error.

Comparison of the data presented in Table 2 and Table 3 shows that the accuracy of the  $Y_p$  series approximation using CSSA method is a bit better than that for the BCA method. Remarkably, that the best RMSE in filling  $Y$  values achieved by both methods ( $0.08''-0.09''$ ) are very close to the  $Y_p$  uncertainty given in the IERS C01 series ( $0.090''$ , which is assumed to be the standard deviation, equivalent to RMSE), confirming both the reality of the IERS C01 errors and the correctness of our error estimate. The gap-filling plots with the best parameters described above are shown in Fig. 4.

Consider the CSSA decomposition components of the time series  $Y$  after filling the actual gap. Recall that the imaginary parts of the complex components are related to the series  $Y$ . The latter for the CSSA 6-component solution with  $L = 119$  are shown in Fig. 5, and Fig. 6 shows the  $Y$  components for the 9-component CSSA solution, as examples.

Table 3: MAE/RMSE filling errors on artificial gaps for SSA model order  $r = 1 \dots 17$ , arcseconds.

$r$	$L=60$			$L=119$			$L=238$		
	1D-SSA	MSSA	CSSA	1D-SSA	MSSA	CSSA	1D-SSA	MSSA	CSSA
1	.125/.150	.117/.145	.104/.129	.121/.143	.114/.142	.104/.130	.121/.143	.114/.142	.106/.135
2	.112/.138	.114/.142	.084/.109	.104/.129	.109/.137	.084/.110	.107/.134	.108/.137	.087/.115
3	.093/.118	.101/.124	.070/.092	.089/.116	.094/.118	.076/.099	.091/.120	.091/.118	.080/.105
4	.081/.107	.102/.124	<b>.066/.085</b>	.082/.109	.090/.113	.072/.094	.085/.113	.086/.112	.076/.099
5	.080/.107	.110/.134	<b>.064/.083</b>	.085/.110	.092/.114	.070/.090	.086/.112	.086/.111	.072/.094
6	.078/.105	.116/.140	.067/.087	.083/.108	.095/.117	<b>.065/.084</b>	.083/.106	.086/.109	.071/.091
7	.081/.109	.124/.150	.067/.088	.085/.111	.101/.123	<b>.064/.084</b>	.084/.106	.087/.109	<b>.066/.085</b>
8	.078/.103	.131/.158	.071/.091	.086/.112	.106/.129	<b>.064/.084</b>	.083/.106	.090/.112	.073/.093
9	.083/.107	.139/.168	.073/.095	.090/.117	.113/.137	<b>.065/.085</b>	.084/.109	.096/.118	.075/.096
10	.086/.111	.144/.174	.077/.099	.088/.113	.116/.139	.068/.090	.085/.109	.100/.122	.076/.097
11	.094/.121	.148/.179	.079/.102	.088/.111	.118/.143	.071/.092	.085/.110	.104/.126	.074/.094
12	.092/.119	.150/.182	.083/.107	.080/.102	.123/.149	.072/.095	.083/.107	.105/.127	.074/.095
13	.095/.124	.152/.184	.085/.110	.081/.106	.129/.156	.073/.097	.084/.108	.108/.130	.076/.098
14	.097/.126	.153/.186	.087/.112	.085/.111	.133/.160	.073/.099	.085/.108	.110/.133	.076/.099
15	.103/.133	.155/.188	.087/.110	.090/.118	.137/.166	.071/.097	.090/.114	.114/.137	.070/.091
16	.105/.136	.156/.189	.085/.107	.093/.121	.140/.169	.075/.102	.086/.110	.116/.139	.070/.091
17	.110/.143	.157/.191	.094/.116	.092/.122	.143/.173	.081/.108	.088/.115	.119/.142	.070/.091

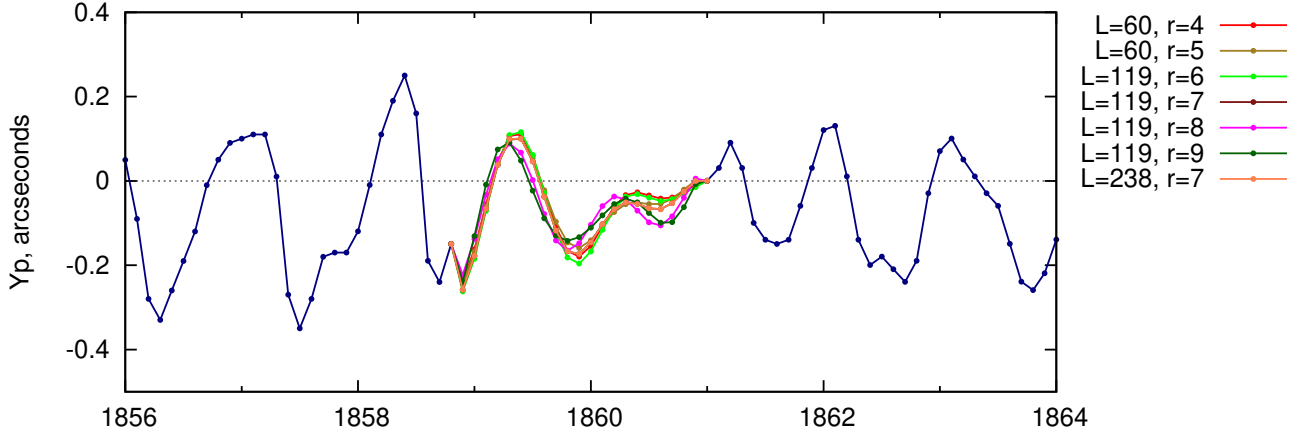


Figure 4: IERS C01  $Y_p$  series with filled missed data between 1858.9 and 1860.9 computed using the CSSA model with the seven models providing the minimal approximation error.

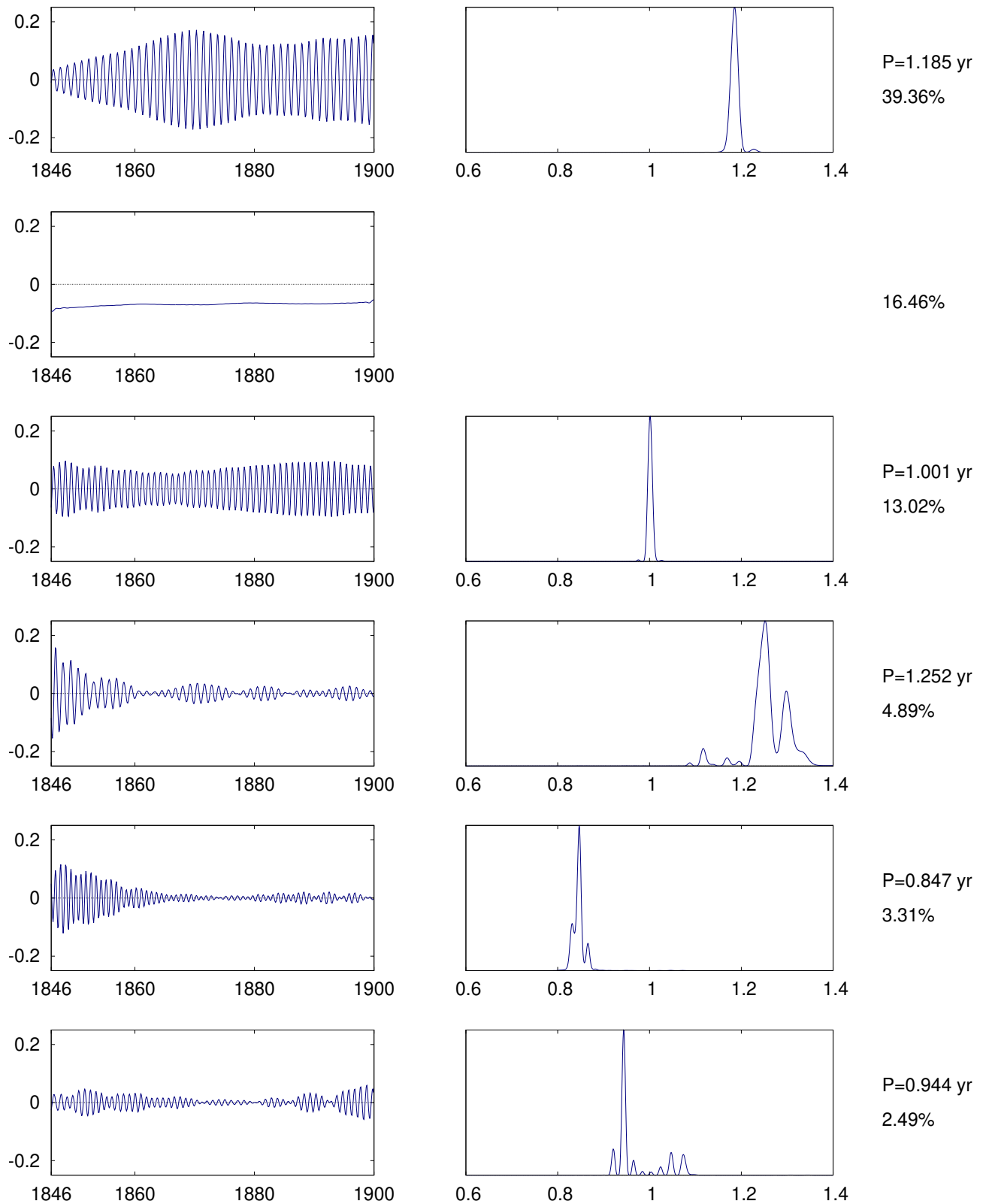


Figure 5: The Y components of CSSA solution with  $r=6$  (in arcseconds) and their Lomb-Scargle periodograms (except the trend component, arbitrary units). The period of the most powerful oscillation and the contribution of the component to the total signal are shown on the right.

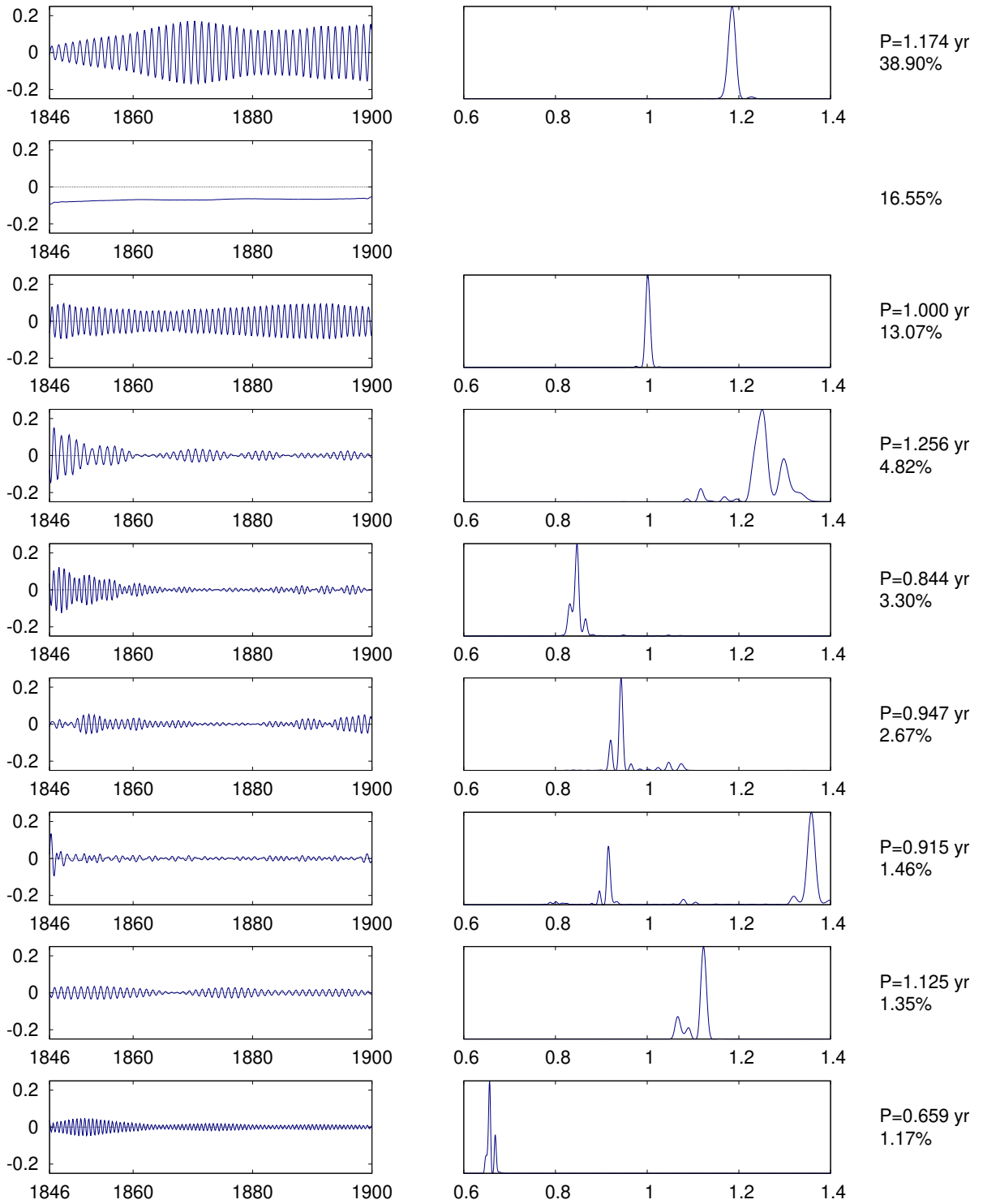


Figure 6: The Y components of CSSA solution with  $r=9$  (in arcseconds) and their Lomb-Scargle periodograms (except the trend component, arbitrary units). The period of the most powerful oscillation and the contribution of the component to the total signal are shown on the right.

It can be seen that the leading six components of the 9-component solution have practically the same periods as those for the 6-component solution. Some components show two spectral peaks, which can be caused by mixing of two periodicities or by phase instability of the component. In all solutions, the first component corresponds to the main CW oscillation, and the third component corresponds to the main AW oscillation. In Figs. 5 and 6, two minor components with periods of 0.847 yr and 0.944 yr can also be seen. The corresponding peaks in Fig. 2 are small, at the noise level. We consider this fact as confirmation of the better sensitivity of the SSA method to small components in the analyzed signal, which allows for their better detection.

Since the imputed values for the seven CSSA models described above provide approximately equal errors on the artificial gaps, the average of these values can be recommended as the final method of filling in the actual gap in the IERS C01 series. This filling method using the average of seven gap fillings has a slightly smaller MAE (0.0628 vs. 0.0638–0.0662) on the considered set of artificial gaps, compared to each of these seven gap fillings.

## 5 Final results

Average results (filling  $Y_p$  values) computed using the BCA and SSA methods are presented in Table 4 with the number of decimal places corresponding to the IERS C01 series. The IERS C01 series with added filling values is shown in Fig. 7.

Both methods show good agreement, especially in the first year of the gap interval, 1859–1860. The agreement in the second year of the interval, 1860–1861, is somewhat worse, but can be considered quite satisfactory, considering that the  $Y_p$  error in the IERS C01 series is  $0.09''$ . Generally speaking, it should be kept in mind that the accuracy of the reconstruction is limited by the accuracy of the IERS C01 data, especially before the gap in the 1840s–1850s.

## 6 Conclusions

In this paper, the first attempt has been made to address the problem of filling the 2-year gap in the IERS C01  $Y_p$  series in 1858.9–1860.9. For this purpose, two methods were proposed and investigated. The first is the LS adjustment of the 9-parameter BCA model, consisting of a bias and two harmonic terms, CW and AW, with linearly changing amplitude, and its modification, the 13-parameter BCA2 model, which includes two CW components. The second method is CSSA (complex SSA), applied to the IERS C01 PM series in complex form, which allows us to obtain a fully data-driven solution, not limited by the parameters of parametric models. Besides, the discrepancies between the results obtained by the two methods may be due to the fact that the parametric models are based on a several times shorter interval than the SSA model. Thus, parametric models mainly describe the local PM behaviour on the date interval around the gap and under the assumption of a linear change in the CW and AW amplitudes, while the SSA model is much less sensitive to a priori assumptions and is more suitable for describing the long-term PM features, which is the primary interest of this paper.

Therefore, we consider the result obtained by SSA as more reliable because it takes into account all the features of the observed PM data and all the main components of its structure, while the parametric model uses only predefined components, which may not adequately describe the results of the observations. However, we present both the results obtained by the BCA and SSA methods in Table 4 so that the user can choose the variant that looks most appropriate for the problem under investigation, or simply use the average of the two.

Table 4: Filled  $Y_p$  values, arcseconds.

Epoch	Model	
	BCA	SSA
1858.9	-0.236505	-0.247675
1859.0	-0.153508	-0.164798
1859.1	-0.050599	-0.053550
1859.2	0.039868	0.045943
1859.3	0.091581	0.100224
1859.4	0.092240	0.095042
1859.5	0.046379	0.038934
1859.6	-0.027558	-0.042570
1859.7	-0.104471	-0.118523
1859.8	-0.161363	-0.164565
1859.9	-0.184487	-0.170918
1860.0	-0.172543	-0.143915
1860.1	-0.135271	-0.101195
1860.2	-0.088418	-0.063027
1860.3	-0.047375	-0.043324
1860.4	-0.021975	-0.044098
1860.5	-0.014260	-0.055752
1860.6	-0.019681	-0.063258
1860.7	-0.030755	-0.055410
1860.8	-0.041278	-0.032369
1860.9	-0.049166	-0.006942

It should be noted that there are many methods for efficiently processing unevenly spaced data, in particular, data with gaps. Many of widely used methods of data analysis, such as LS adjustment, spectral analysis, SSA, wavelet technique, etc., have modifications for processing unevenly spaced data. Many examples of application of such analyses to study PM series can be found in the literature, e. g., Gaposchkin (1972); Kołaczek and Kosek (1999); Gambis (2000); Guo et al. (2005); Zotov and Bizouard (2012); Beutler et al. (2020); Lopes et al. (2022). However, the missing two years of  $Y_p$  data may introduce bias in PM modeling if inappropriate analysis methods are used. Our work aims to provide interested users with the option to work with evenly distributed data and to use appropriate mathematical methods, if they want. In most cases, one cannot expect a significant difference in the results obtained with original and filled series, but working with evenly spaced data is more convenient and allows for detailed epoch-by-epoch analysis. Including the proposed filling values into the IERS C01 series (indeed, with corresponding note) will provide full continuous, evenly spaced PM series over the entire date range starting from 1846. This will also allow to avoid (even small) mistakes in using this series for scientific analysis if the gap in the series in its current, formally evenly spaced form is not properly taken into account. Perhaps for this reason, e. g., Schuh et al. (2001) and Vondrák (1988) started their analysis from 1861.0.

In this study, mathematical methods were mainly used to complete the existing IERS C01 PM series by filling in the missing  $Y_p$  values for 21 epochs in the period 1858.9 to 1860.9. On the other hand, mining and reprocessing historical observations looks very interesting, but this huge task goes

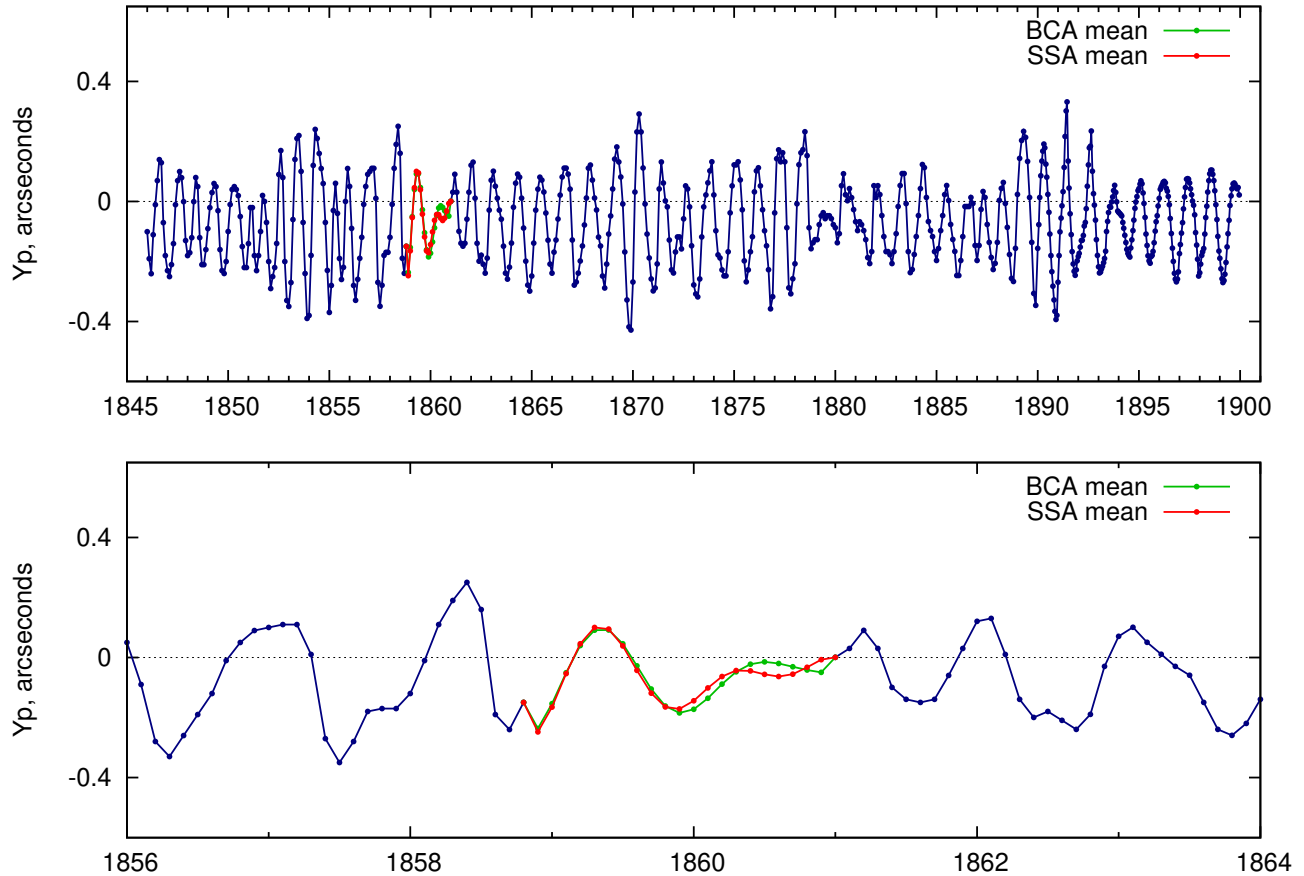


Figure 7: IERS C01  $Y_p$  series with filled missed data between 1858.9 and 1860.9 using the average values for both BCA and SSA models.

far beyond the scope of this paper and will obviously require cooperation between observatories that could preserve in their archives declination and latitude observations carried out in the 19th century. Therefore, attempts to improve the quality of the IERS C01 series in the 19th century should be considered, in our opinion, an actual task.

## Appendix A Filling the gaps with SSA

Suppose there is a method that knows how to remove noise from a noisy signal. Then we can propose a simple iterative gap-filling method. First, the places with missing values are filled with some initial values, e. g., the mean of the series, then the signal extraction is performed, the obtained signal estimates are put at the gaps, the signal extraction method is applied again, and so the procedure is repeated until convergence.

Typically, the signal estimation method has some parameters. Then the approach is as follows. An artificial gap is placed in the part of the series  $Y$  that does not contain gaps and the parameters are chosen so that the gap filling error is minimized. For the stability of the result, the error of gap filling is calculated for different locations of gaps and the errors are averaged. It is natural to choose the type of artificial gaps the same as the actual one. For example, if the actual gap consists of consecutive

missing values and has length  $M$ , then artificial gaps should be the same.

**Algorithm 1** (Finding the filling error on artificial gaps):

*Input parameters:* time series  $\mathbf{Y}$  with a gap, length  $M$  of artificial gap interval, set of intervals with artificial gaps of size  $R$ , measure of filling errors.

1. Take an interval of length  $M$  from the set of artificial gaps and replace the values of the series  $\mathbf{Y}$  in this interval by missing values.
2. Fill the artificial gap from step 1 together with the actual one using iterative gap filling.
3. Calculate the error between the values imputed in step 2 for artificial gaps and the actual values of the series  $\mathbf{Y}$  in the corresponding interval.
4. Repeat steps 1–3  $R$  times for the given set of  $R$  intervals of artificial missing values. For each interval, the error is calculated according to step 3.

*Result:* The arithmetic average of the  $R$  errors computed in step 4.

In this paper, we use SSA (Golyandina et al., 2001; Golyandina and Zhigljavsky, 2020) as the signal reconstruction (noise removal) method that is part of the iterative gap-filling process (Kondrashov and Ghil, 2006). Let us describe it briefly. The SSA method in its version for signal extraction has only two parameters, the window length  $L$  and the number of components  $r$ . At the first stage, the time series  $\mathbf{X} = (x_1, \dots, x_N)$  is transformed into the so-called trajectory matrix:

$$\mathbf{X} = \begin{pmatrix} x_1 & x_2 & \dots & x_K \\ x_2 & \ddots & \ddots & x_{K+1} \\ \vdots & \ddots & \ddots & \vdots \\ x_L & x_{L+1} & \dots & x_N \end{pmatrix} \quad (5)$$

using the parameter  $L$ . Next, the singular value decomposition (SVD) of the trajectory matrix is constructed. Let  $\mathbf{S} = \mathbf{X}\mathbf{X}^T$ ,  $\lambda_1, \dots, \lambda_L$  be the eigenvalues of the matrix  $\mathbf{S}$  taken in non-increasing order,  $U_1, \dots, U_L$  be the orthonormalized system of eigenvectors corresponding to these eigenvalues. Let  $d = \max\{k : \lambda_k > 0\}$  and  $V_k = \mathbf{X}^T U_k / \sqrt{\lambda_k}$ ,  $k = 1, \dots, d$ . Then the SVD of the matrix  $\mathbf{X}$  can be represented as a sum of elementary matrices:

$$\mathbf{X} = \mathbf{X}_1 + \dots + \mathbf{X}_d, \quad (6)$$

where  $\mathbf{X}_k = \sqrt{\lambda_k} U_k V_k^T$ ,  $k = 1, \dots, d$ .

In the second step, the first  $r$  elementary matrices of the SVD are summed:

$$\mathbf{Y} = \mathbf{X}_1 + \dots + \mathbf{X}_r, \quad (7)$$

and their sum is converted into a time series

$$\tilde{y}_s = \sum_{(l,k) \in A_s} y_{lk} / |A_s|, \quad (8)$$

where  $y_{lk}$  are the elements of the matrix  $\mathbf{Y}$ , the sets  $A_s = \{(l, k) : l + k = s + 1, 1 \leq l \leq L, 1 \leq k \leq K\}$ ,  $s = 1, \dots, N$ , give the indices corresponding to the elements on the side diagonals,  $|A_s|$  denotes the

number of elements in the sets  $A_s$ . The time series  $\tilde{Y} = (\tilde{y}_1, \dots, \tilde{y}_N)$  is considered as the SSA estimate of the signal.

The SSA algorithm can be extended to the simultaneous analysis of two time series,  $X$  and  $Y$ , in two forms. In the case of Complex SSA (CSSA) for a time series of the form  $x_n + iy_n$ ,  $n = 1, \dots, N$ , the transpose operator  $T$  is replaced by the Hermite conjugate operator  $H$ . The complex form of SSA has been considered since its origin. In the complex form, the first descriptions of the method can be found, for example, in Kumaresan and Tufts (1982); Keppenne and Lall (1996).

In the case of Multivariate SSA (MSSA) for two time series of the  $(x_n, y_n)$ ,  $n = 1, \dots, N$ , the difference lies in the construction of the trajectory matrix, which consists of stacked trajectory matrices of the time series. A more detailed description can be found in Golyandina et al. (2015).

## Acknowledgments

The authors are grateful to three anonymous reviewers and scientific editor, Alberto Ecsapa, for valuable comments and suggestions which helped to improve the manuscript. The SSA data analysis was performed using the package `Rssa`, <https://CRAN.R-project.org/package=Rssa>. This research has made use of SAO/NASA Astrophysics Data System (ADS), <https://ui.adsabs.harvard.edu/>. The figures were prepared using `gnuplot`, <http://www.gnuplot.info/>.

## Author Contributions

Z.M. designed the paper and performed preliminary data analysis and computations related to the parametric model. N.G. and R.O. performed the SSA data analysis. All authors contributed to the writing of the text, discussed the results, and approved the manuscript for submission.

## Data Availability

IERS C01 EOP series is available at <https://datacenter.iers.org/eop.php> and <ftp://hpiers.obspm.fr/>.

## Conflicts of interest

The authors state that there are no known conflicts of interest.

## References

- Beutler G, Villiger A, Dach R, Verdun A, Jäggi A (2020) Long polar motion series: Facts and insights. *Advances in Space Research* 66(11):2487–2515. <https://doi.org/10.1016/j.asr.2020.08.033>
- Bizouard C, Lambert S, Gattano C, Becker O, Richard JY (2019) The IERS EOP 14C04 solution for Earth orientation parameters consistent with ITRF 2014. *Journal of Geodesy* 93(5):621–633. <https://doi.org/10.1007/s00190-018-1186-3>
- Chandler SC (1894a) On the inequalities in the coefficients of the law of latitude-variation. *AJ* 14:73–75. <https://doi.org/10.1086/102074>

- Chandler SC (1894b) Variation of latitude from the Greenwich muralcircle Observations, 1836-51. *AJ* 14:57–60. <https://doi.org/10.1086/102062>
- Dick S, McCarthy D, Luzum B (eds) (2000) IAU Colloq. 178: Polar Motion: Historical and Scientific Problems, *Astronomical Society of the Pacific Conference Series*, vol 208. Astronomical Society of the Pacific
- Elsner JB, Tsonis AA (1996) *Singular Spectrum Analysis: A New Tool in Time Series Analysis*. Springer
- Fedorov EP, Korsun' AA, Major SP, Panchenko NI, Taradij VK, Yatskiv YS (1972) Motion of the Earth's pole from 1890.0 to 1969.0. *Kyiv, Naukova Dumka*
- Gambis D (2000) Long-term Earth Orientation Monitoring Using Various Techniques. In: Dick S, McCarthy D, Luzum B (eds) IAU Colloq. 178: Polar Motion: Historical and Scientific Problems, *Astronomical Society of the Pacific, Astronomical Society of the Pacific Conference Series*, vol 208, pp 337–344
- Gaposchkin EM (1972) Analysis of Pole Position from 1846 to 1970. In: Melchior P, Yumi S (eds) IAU Symp. 48: Rotation of the Earth, Cambridge University Press, vol 48, p 19–32, <https://doi.org/10.1017/S0074180900098016>
- Ghil M, Allen MR, Dettinger MD, Ide K, Kondrashov D, Mann ME, Robertson AW, Saunders A, Tian Y, Varadi F, Yiou P (2002) Advanced Spectral Methods for Climatic Time Series. *Reviews of Geophysics* 40(1):1003. <https://doi.org/10.1029/2000RG000092>
- Golyandina N, Osipov E (2007) The “Caterpillar”–SSA method for analysis of time series with missing values. *J Stat Plan Inference* 137(8):2642–2653. <https://doi.org/10.1016/j.jspi.2006.05.014>
- Golyandina N, Zhigljavsky A (2020) *Singular Spectrum Analysis for Time Series*. Second Edition. Springer, <https://doi.org/10.1007/978-3-662-62436-4>
- Golyandina N, Nekrutkin V, Zhigljavsky A (2001) *Analysis of Time Series Structure: SSA and related techniques*. Chapman and Hall/CRC
- Golyandina N, Korobeynikov A, Shlemov A, Usevich K (2015) Multivariate and 2D Extensions of Singular Spectrum Analysis with the Rssa Package. *J Stat Softw* 67(2):1–78. <https://doi.org/10.18637/jss.v067.i02>
- Guo JY, Greiner-Mai H, Ballani L, Jochmann H, Shum CK (2005) On the double-peak spectrum of the Chandler wobble. *Journal of Geodesy* 78(11-12):654–659. <https://doi.org/10.1007/s00190-004-0431-0>
- Höpfner J (2004) Low-Frequency Variations, Chandler and Annual Wobbles of Polar Motion as Observed Over One Century. *Surveys in Geophysics* 25(1):1–54. <https://doi.org/10.1023/B:GEOP.0000015345.88410.36>
- Ji K, Shen Y, Chen Q, Wang F (2023) Extended singular spectrum analysis for processing incomplete heterogeneous geodetic time series. *Journal of Geodesy* 97(8):74. <https://doi.org/10.1007/s00190-023-01764-8>

- Keppenne C, Lall U (1996) Complex singular spectrum analysis and multivariate adaptive regression splines applied to forecasting the southern oscillation. *Experimental Long-Lead Bulletin* 5(3):39–40
- Kołodziej B, Kosek W (1999) Variations of the amplitude of the Chandler wobble. In: *Journées 1998 “Systèmes de Référence Spatio-Temporels: Conceptual, Conventional and Practical Studies Related to Earth Rotation”*, pp 215–220
- Kondrashov D, Ghil M (2006) Spatio-temporal filling of missing points in geophysical data sets. *Nonlinear Processes in Geophysics* 13(2):151–159. <https://doi.org/10.5194/npg-13-151-2006>
- Kumaresan R, Tufts D (1982) Estimating the parameters of exponentially damped sinusoids and pole-zero modeling in noise. *IEEE Trans Acoust* 30(6):833–840
- Lopes F, Courtillot V, Gibert D, Le Mouél JL (2022) Extending the Range of Milankovic Cycles and Resulting Global Temperature Variations to Shorter Periods (1–100 Year Range). *Geosciences* 12(12):448. <https://doi.org/10.3390/geosciences12120448>
- Malkin Z, Miller N (2010) Chandler wobble: two more large phase jumps revealed. *Earth, Planets and Space* 62(12):943–947. <https://doi.org/10.5047/eps.2010.11.002>
- Miller NO (2011) Chandler wobble in variations of the Pulkovo latitude for 170 years. *Solar System Research* 45(4):342–353. <https://doi.org/10.1134/S0038094611040058>
- Okhotnikov G, Golyandina N (2019) EOP time series prediction using singular spectrum analysis. In: Corpetti T, Ienco D, Interdonato R, et al (eds) *Proceedings of MACLEAN: MACHINE Learning for EARTH ObservatioN Workshop*, RWTH Aachen University, Germany, CEUR Workshop Proceedings, Vol. 2466
- Orlov AY (1961) *Selected works*, Vol. 1. Kyiv: Academy of Sciences of Ukraine
- Rykhlova LV (1970a) The coordinates of the Earth’s pole for the years 1846.0–1891.5. *Soobshcheniya Gosudarstvennogo Astronomicheskogo Instituta, Moscow State University* 163:3–10
- Rykhlova LV (1970b) Variations of the Washington latitude in 1845–1891. *Trudy Gosudarstvennogo Astronomicheskogo Instituta, Moscow State University* 39:200–212
- Rykhlova LV, Kurbasova GS (1990) The Study of the Structure of 142-Year Series of Pole Coordinates. In: Lieske JH, Abalakin VK (eds) *Inertial Coordinate System on the Sky*, vol 141, p 157
- Schuh H, Nagel S, Seitz T (2001) Linear drift and periodic variations observed in long time series of polar motion. *Journal of Geodesy* 74(10):701–710. <https://doi.org/10.1007/s001900000133>
- Seitz F, Kirschner S, Neubersch D (2012) Determination of the Earth’s pole tide Love number  $k_2$  from observations of polar motion using an adaptive Kalman filter approach. *Journal of Geophysical Research (Solid Earth)* 117(B9):B09403. <https://doi.org/10.1029/2012JB009296>
- Shen Y, Peng F, Li B (2015) Improved singular spectrum analysis for time series with missing data. *Nonlinear Processes in Geophysics* 22(4):371–376. <https://doi.org/10.5194/npg-22-371-2015>. <https://doi.org/10.5194/npgd-1-1947-2014>
- Thackeray WG (1893) Latitude variation and Greenwich observations, 1851–91. *MNRAS* 53:120. <https://doi.org/10.1093/mnras/53.3.120>

- Vautard R, Ghil M (1989) Singular spectrum analysis in nonlinear dynamics, with applications to paleoclimatic time series. *Physica D Nonlinear Phenomena* 35:395–424. [https://doi.org/10.1016/0167-2789\(89\)90077-8](https://doi.org/10.1016/0167-2789(89)90077-8)
- Vityazev VV, Miller NO, Prudnikova EJ (2010) Singular Spectrum Analysis in Astrometry and Geodynamics. In: de León M, de Diego DM, Ros RM (eds) *Mathematics and Astronomy: A Joint Long Journey*, AIP, American Institute of Physics Conference Series, vol 1283, pp 319–328, <https://doi.org/10.1063/1.3506397>
- Vondrák J (1988) Is Chandler Frequency Constant? In: Babcock AK, Wilkins GA (eds) *The Earth's Rotation and Reference Frames for Geodesy and Geodynamics*, IAU Symposium, vol 128, p 359
- Vondrák J, Ron C, Pešek I, Čeppek A (1995) New global solution of Earth orientation parameters from optical astrometry in 1900-1990. *A&A* 297:899–906
- Vondrák J, Ron C, Štefka A (2010) Earth orientation parameters based on EOC-4 astrometric catalog. *Acta Geodyn Geomater* 7(3):245–251
- Yamaguchi R, Furuya M (2024) Can we explain the post-2015 absence of the Chandler wobble? *Earth, Planets and Space* 76(1):1. <https://doi.org/10.1186/s40623-023-01944-y>
- Yatskiv Y (2000) Chandler Motion Observations. In: Dick S, McCarthy D, Luzum B (eds) *IAU Colloq. 178: Polar Motion: Historical and Scientific Problems*, Astronomical Society of the Pacific, Astronomical Society of the Pacific Conference Series, vol 208, pp 383–395
- Yi S, Sneeuw N (2021) Filling the Data Gaps Within GRACE Missions Using Singular Spectrum Analysis. *Journal of Geophysical Research (Solid Earth)* 126(5):e2020JB021227. <https://doi.org/10.1029/2020JB021227>
- Zechmeister M, Kürster M (2009) The generalised Lomb-Scargle periodogram. A new formalism for the floating-mean and Keplerian periodograms. *A&A* 496(2):577–584. <https://doi.org/10.1051/0004-6361:200811296>
- Zotov L, Bizouard C (2012) On modulations of the Chandler wobble excitation. *Journal of Geodynamics* 62:30–34. <https://doi.org/10.1016/j.jog.2012.03.010>
- Zotov LV (2010) Dynamical Modeling and Excitation Reconstruction as Fundamental of Earth Rotation Prediction. *Artificial Satellites* 45(2):95–106. <https://doi.org/10.2478/v10018-010-0010-y>
- Zotov LV, Sidorenkov NS, Bizouard C (2022) Anomalies of the Chandler Wobble in 2010s. *Moscow University Physics Bulletin* 77(3):555–563. <https://doi.org/10.3103/S0027134922030134>